

# Graph Neural Networks for Decentralized Multi-Robot Path Planning

Qingbiao Li<sup>1</sup>, Fernando Gama<sup>2</sup>, Alejandro Ribeiro<sup>2</sup>, Amanda Prorok<sup>1</sup>

## ABSTRACT

Efficient and collision-free navigation in multi-robot systems is fundamental to advancing mobility. Scenarios where the robots are restricted in observation and communication range call for decentralized solutions, whereby robots execute localized planning policies. From the point of view of an individual robot, however, its local decision-making system is incomplete, since other agents' unobservable states affect future values. *The manner in which information is shared is crucial to the system's performance, yet is not well addressed by current approaches.* To address these challenges, we propose a combined architecture, with the goal of learning a decentralized sequential action policy that yields efficient path plans for all robots. Our framework is composed of a convolutional neural network (CNN) that extracts adequate features from local observations, and a graph neural network (GNN) that communicates these features among robots. We train the model to imitate an expert algorithm, and use the resulting model online in decentralized planning involving only local communication. We evaluate our method in simulations involving teams of robots in cluttered workspaces. We measure the success rates and sum of costs over the planned paths. The results show a performance close to that of our expert algorithm, demonstrating the validity of our approach. In particular, we show our model's capability to generalize to previously unseen cases (involving larger environments and larger robot teams).

## KEYWORDS

Multi-Agent Path Finding; Decentralized Planning; Deep Learning; Graph Neural Networks;

## 1 INTRODUCTION

Efficient and collision-free navigation in multi-robot systems is fundamental to advancing mobility. The problem, generally referred to as Multi-Robot Path Planning (MRPP) or Multi-Agent Path Finding (MAPF), aims at generating collision-free paths leading robots from their origins to designated destinations. Solutions to this problem lend themselves to search and rescue operations [15], product pickup and delivery [12], item retrieval in warehouses [6], and mobility-on-demand services [20, 33]. Current approaches can be classified as either *coupled* or *decoupled*, depending on the structure of the state space that is searched. While coupled approaches are able to ensure the optimality and completeness of the solution, they involve *centralized* components, and tend to scale poorly with the number of robots [32, 34]. Decoupled approaches, on the other

hand, compute trajectories for each robot separately, and re-plan only in case of conflicts [37, 39, 41]. This can significantly reduce the computational complexity of the planning task, but generally produces sub-optimal and incomplete solutions. It is noteworthy, however, that decoupled approaches lend themselves naturally to *decentralized* solutions. Balancing optimality and completeness with the complexity of computing a solution, however, is still an open research problem [2, 25].

This work focuses on multi-robot path planning for scenarios where the robots are restricted in observation and communication range. This naturally arises when considering physical robots equipped with hardware constraints that limit their perception and communication capabilities [16]. These scenarios impose a decentralized structure, where at any given point in time, robots have only partial information of the system state. This condition requires adapted control algorithms. In this paper, we propose a combined architecture, where we train a convolutional neural network (CNN) that extracts adequate features from local observations, and a graph neural network (GNN) to communicate these features among robots [10] with the ultimate goal of learning a decentralized sequential action policy that yields efficient path plans for all robots. The GNN implementation seamlessly adapts to the partial information structure of the problem, since it is computed in a decentralized manner. We train this architecture to imitate an optimal coupled planner with global information that is available offline at training time. We utilize a dataset aggregation method that leverages an online expert to resolve hard cases, thus expediting the learning process. The resulting trained model is used online in an efficient, decentralized manner, involving communication only with nearby robots. Furthermore, we show that the model can be deployed on much larger robot teams than the ones it was trained on.

This paper is organized as follows. In Sec. 2, we discuss related work and in Sec. 3, we formulate the problem. We then introduce fundamental concepts of graph signal processing and graph convolutions in Sec. 4, so that GNNs can be formally defined in Sec. 4.2. Sec. 5 presents the proposed architecture, and its core components. Finally, Sec. 6 summarizes our experimental setup and results, and is followed by a discussion in Sec. 7. Conclusions are drawn in Sec. 8.

## 2 RELATED WORK

Classical approaches to multi-robot path planning can generally be described as either centralized (assuming the existence of a central component that knows the state of the whole robot system) or decentralized (where no single component has the full picture, but cooperation must still be achieved). *Centralized* approaches are facilitated by a planning unit that monitors all robots' positions and desired destinations, and returns a coordinated plan of trajectories (or way-points) for all the robots in the system. These plans are communicated to the respective robots, which use them for real-time

<sup>1</sup>Qingbiao Li and Amanda Prorok are with the Department of Computer Science and Technology, University of Cambridge, Cambridge, United Kingdom (Emails: ql295, asp45@cam.ac.uk).

<sup>2</sup>Fernando Gama and Alejandro Ribeiro are with the Department of Electrical and Systems Engineering, University of Pennsylvania, Philadelphia, USA (Emails: fgama, aribeiro@seas.upenn.edu).

on-board control of their navigation behavior. Coupled centralized approaches, which consider the joint configuration space of all involved robots, have the advantage of producing optimal and complete plans, yet tend to be computationally very expensive [28]. Indeed, solving for optimality is NP-hard [42], and although significant progress has been made towards alleviating the computational load [8, 29, 43], these approaches still scale poorly in environments with a high number of potential path conflicts.

*Decentralized* approaches provide an attractive alternative to centralized approaches, firstly, because they reduce the computational overhead, and secondly, because they relax the dependence on centralized units. This body of work considers the generation of collision-free paths for individual robots that cooperate only with immediate neighbors [4, 41], or with no other robots at all [1, 38]. In the latter case, coordination is reduced to the problem of reciprocally avoiding other robots (and obstacles), and can generally be solved without the use of communication. Yet, by taking purely local objectives into account, global objectives (such as path efficiency) cannot be explicitly optimized. In the former case, it has been shown that monotonic cost reduction of global objectives can be achieved. This feat, however, relies on strong assumptions (e.g., problem convexity and invariance of communication graph [23, 40]) that can generally not be guaranteed in real robot systems.

*Learning-based* methods have proven effective at designing robot control policies for an increasing number of tasks [21, 35]. The application of learning-based methods to multi-robot motion planning has attracted particular attention due to their capability of handling high-dimensional joint state-space representations, by offloading the online computational burden to an offline learning procedure. The work in [7] proposes a decentralized multi-agent collision avoidance algorithm based on deep reinforcement learning. Their results show that significant improvement in the quality of the path (i.e., time to reach the goal) can be achieved with respect to current benchmark algorithms (e.g., ORCA [38]). Also in recent work, Sartoretti et al. [26] propose a hybrid learning-based method for multi-agent path-finding that uses both imitation learning (based on an expert algorithm) and multi-agent reinforcement learning. Robots controlled by this method perform well in various team sizes in low obstacle densities. It is note-worthy that none of the aforementioned learning-based approaches consider inter-robot communication, and thus, do not exploit the scalability benefits of fully decentralized approaches. Learning what, how, and when to communicate is key to this aim.

Of particular interest to us is the capability of learning-based methods to handle high-dimensional joint state-space representations, useful when planning for large-scale collective robotic systems, by offloading the online computational burden to an offline learning procedure [7, 36]. Key to this learning procedure is the fact that each robot must be able to accumulate information from other robots in its neighborhood. From the point of view of an individual robot, its local decision-making system is incomplete, since other agents' unobservable states affect future values. *The manner in which information is shared is crucial to the system's performance, yet is not well addressed by current machine learning approaches.* Graph Neural Networks (GNNs) promise to overcome this deficiency [10, 27]. They capture the *relational* aspect of robot communication and coordination by modeling the collective

robot system as a graph: each robot is a node, and edges represent communication links [19]. Although GNNs have been applied to a number of problem domains, including molecular biology [5], quantum chemistry [11], and simulation engines [3], they have only very recently been considered within the multi-robot domain [19, 36].

**Contributions.** The application of GNNs to the problem of multi-robot path planning is novel. GNNs offer an efficient architecture that operates in a localized manner, where information is shared over a multi-hop communication network, through communication with nearby neighbors only [10]. Our key contribution in this work is the development of a framework that can learn what information needs to be shared between robots to facilitate efficient path planning. This framework is composed of a convolutional neural network (CNN) that extracts adequate features from local observations, and a graph neural network (GNN) that learns to communicate these features among robots. By jointly training these two components, the system is able to best determine what information is relevant for the team as a whole, and share this. The proposed model is trained to imitate a centralized coupled planner, and makes use of a dataset aggregation method that leverages an online expert to resolve hard cases, thus expediting the learning process. Our aim is to achieve comparable performance in terms of success rate and flowtime (sum of path costs), while also being able to generalize to previously unseen cases, such as larger robot teams and environments.

### 3 PROBLEM FORMULATION

Let  $\mathcal{V} = \{v_1, \dots, v_N\}$  be the set of  $N$  robots. At time  $t$ , each robot perceives its surroundings within a given field of vision, and knows where its own target destination is located. This map perceived by robot  $i$  is denoted by  $\mathbf{Z}_t^i \in \mathbb{R}^{W_{FOV} \times H_{FOV}}$  where  $W_{FOV}$  and  $H_{FOV}$  are the width and height, respectively, and are determined by the field of vision radius  $\rho$ .

The robots can communicate with each other as determined by the communication network. We can describe this network at time  $t$  by means of a graph  $\mathcal{G}_t = (\mathcal{V}, \mathcal{E}_t, \mathcal{W}_t)$  where  $\mathcal{V}$  is the set of robots,  $\mathcal{E}_t \subseteq \mathcal{V} \times \mathcal{V}$  is the set of edges and  $\mathcal{W}_t : \mathcal{E}_t \rightarrow \mathbb{R}$  is a function that assigns weights to the edges. Robots  $v_i$  and  $v_j$  can communicate with each other at time  $t$  if  $(v_i, v_j) \in \mathcal{E}_t$ . The corresponding edge weight  $\mathcal{W}_t(v_i, v_j) = w_t^{ij}$  can represent the strength of the communication (or be equal to 1 if we are only modeling whether there is a link or not).

In this work, we formulate the multi-agent path planning problem as a sequential decision making problem, that each robot solves at every time instant  $t$  with the objective of reaching its destination. More formally, the objective of this work is to learn a mapping  $\mathcal{F}$  that takes the maps  $\{\mathbf{Z}_t^i\}_{v_i \in \mathcal{V}}$  and the communication network  $\mathcal{G}_t$  at time  $t$  and determines an appropriate action  $\mathbf{u}_t$ . We want the action  $\mathbf{u}_t = \mathcal{F}(\{\mathbf{Z}_t^i\}, \mathcal{G}_t)$  to be such that it contributes to the global objective of moving the robots towards their destinations in the shortest possible time while avoiding collisions with other robots and with obstacles that might be present. The mapping  $\mathcal{F}$  has to be restricted to involve communication only among nearby robots, as dictated by the network  $\mathcal{G}_t$  at each time instant  $t$ . Finally, note that

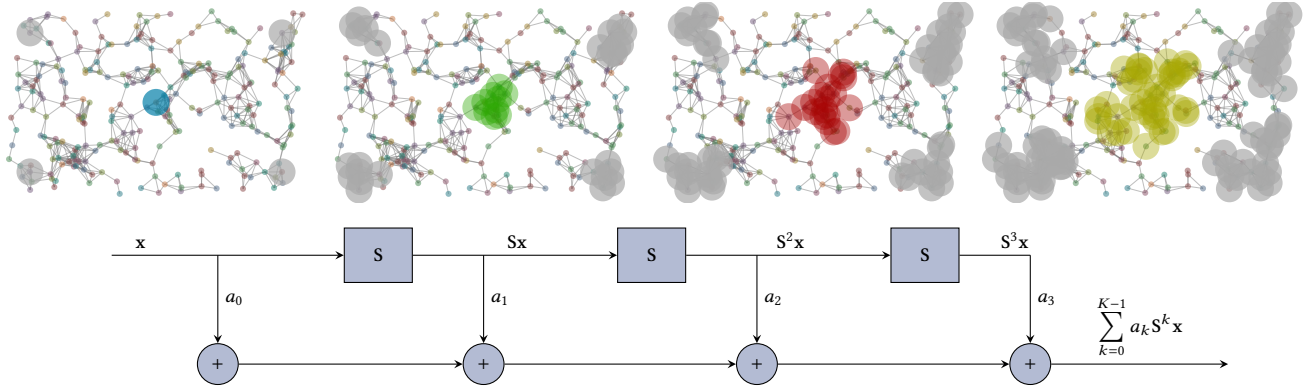


**Figure 1:** Graph convolution. Every node takes its data value  $x$  and weighs it by  $a_0$  (first graph). Then, all the nodes exchange information with their one-hop neighbors to build  $Sx$ , and weigh the result by  $a_1$  (second graph). Next, they exchange their values of  $Sx$  again to build  $S^2x$  and weigh it by  $a_2$  (third graph). This procedure continues for  $K$  steps until all  $a_k S^k x$  have been computed for  $k = 0, \dots, K-1$ , and added up to obtain the output of the graph convolution operation (3). To avoid cluttering, this operation is illustrated on only 5 nodes. In each case, the corresponding neighbors accessed by successive relays of information are indicated by the colored disks.

for scalability, the mapping  $\mathcal{F}$  cannot depend on time  $t$ , allowing the system to process sequences of arbitrary duration.

## 4 GRAPH NEURAL NETWORKS

To guarantee that the mapping  $\mathcal{F}$  is restricted to communications only among nearby robots, we parametrize it by means of a GNN, which is a naturally decentralized solution (Sec. 4.2). We then train this GNN to learn appropriate actions that contribute to the global objective by means of supervised learning through an expert algorithm (i.e., imitation learning) (Sec. 5.5).

### 4.1 Graph Convolutions

Assume that each robot has access to  $F$  observations  $\tilde{x}_t^i \in \mathbb{R}^F$  at time  $t$ . Let  $X_t \in \mathbb{R}^{N \times F}$  be the observation matrix where each row collects these  $F$  observations at each robot  $\tilde{x}_t^i$ ,  $i = 1, \dots, N$ ,

$$X_t = \begin{bmatrix} (\tilde{x}_t^1)^\top \\ \vdots \\ (\tilde{x}_t^N)^\top \end{bmatrix} = \begin{bmatrix} \mathbf{x}_t^1 & \dots & \mathbf{x}_t^F \end{bmatrix}. \quad (1)$$

Note that the columns  $\mathbf{x}_t^f \in \mathbb{R}^N$  represent the collection of the observation  $f$  across all nodes, for  $f = 1, \dots, F$ . This vector  $\mathbf{x}_t^f$  is a *graph signal* [17], since it assigns a scalar value to each node,  $\mathbf{x}_t^f : \mathcal{V} \rightarrow \mathbb{R}$  so that  $[\mathbf{x}_t^f]_i = x_t^{if} \in \mathbb{R}$ .

To formally describe the communication between neighboring agents, we need a concise way of describing the graph and relating it to the observations  $X_t$ . Let  $S_t \in \mathbb{R}^{N \times N}$  be a matrix description of  $\mathcal{G}_t$ . That is,  $S_t$  is such that  $[S_t]_{ij} = s_t^{ij} = 0$  if  $(v_j, v_i) \notin \mathcal{E}_t$ . Matrix  $S_t$  thus respects the sparsity of the graph and is called a *graph shift operator* (GSO) [17]. Examples of GSO typically used in the literature include the adjacency matrix of the graph [24], the Laplacian matrix [31], the Markov matrix [13], among others.

The operation  $S_t X_t$  represents a linear combination of neighboring values of the signal due to the sparsity pattern of  $S_t$ . More

precisely, note that the value at node  $i$  for observation  $f$  after operation  $S_t X_t \in \mathbb{R}^{N \times F}$  becomes

$$[S_t X_t]_{if} = \sum_{j=1}^N [S_t]_{ij} [X_t]_{jf} = \sum_{j: v_j \in \mathcal{N}_i} s_t^{ij} x_t^{jf} \quad (2)$$

where  $\mathcal{N}_i = \{v_j \in \mathcal{V} : (v_j, v_i) \in \mathcal{E}_t\}$  is the set of nodes  $v_j$  that are neighbors of  $v_i$ . Note that the second equality in (2) holds because  $s_t^{ij} = 0$  for all  $j \notin \mathcal{N}_i$ .

The linear operation  $S_t X_t$  is essentially *shifting* the values of  $X_t$  through the nodes, since the application of  $S_t$  updates the value at each node by a linear combination of values in the neighborhood. With the shifting operation in place, we can define a *graph convolution* [10] as linear combination of shifted versions of the signal

$$\mathcal{A}(X_t; S_t) = \sum_{k=0}^{K-1} S_t^k X_t A_k \quad (3)$$

where  $\{A_k\}$  is a set of  $F \times G$  matrices representing the filter coefficients combining different observations. Several noteworthy comments are in order with respect to (3). First, multiplications to the left of  $X_t$  need to respect the sparsity of the graph since these multiplications imply combinations across different nodes. Multiplications to the right, on the other hand, can be arbitrary, since they imply linear combination of observations within the same node in a weight sharing scheme. Second,  $S_t^k X_t = S_t (S_t^{k-1} X_t)$  is computed by means of  $k$  communication exchanges with 1-hop neighbors, and is actually computing a summary of the information located at the  $k$ -hop neighborhood. Therefore, the graph convolution is an entirely local operation in the sense that its implementation is naturally distributed. Third, the graph convolution is actually computing the output of a bank of  $FG$  filters where we take as input  $F$  observations per node and combine them to output  $G$  observations per node,  $\mathcal{A}(X_t; S_t) \in \mathbb{R}^{N \times G}$ . There are  $FG$  graph filters involved in (3) each one consisting of  $K$  filter taps, i.e., the  $(f, g)$  filter can

be described by filter taps  $\mathbf{a}^{fg} = [a_0^{fg}, \dots, a_{K-1}^{fg}] \in \mathbb{R}^K$  and these filter taps are collected in the matrix  $\mathbf{A}_k$  as  $[\mathbf{A}_k]_{fg} = a_k^{fg}$ .

## 4.2 Graph Neural Networks

A convolutional GNN [10] consists of a cascade of  $L$  layers, each of which applies a graph convolution (3) followed by a pointwise nonlinearity  $\sigma : \mathbb{R} \rightarrow \mathbb{R}$  (also known as activation function)

$$\mathbf{X}_\ell = \sigma[\mathcal{A}_\ell(\mathbf{X}_{\ell-1}; \mathbf{S})] \quad \text{for } \ell = 1, \dots, L \quad (4)$$

where, in a slight abuse of notation,  $\sigma$  is applied to each element of the matrix  $\mathcal{A}_\ell(\mathbf{X}_{\ell-1}; \mathbf{S})$ . The input to each layer is a graph signal consisting of  $F_{\ell-1}$  observations and the output has  $F_\ell$  observations so that  $\mathbf{X}_\ell \in \mathbb{R}^{N \times F_\ell}$ . The input to the first layer is  $\mathbf{X}_0 = \mathbf{X}_t$  so that  $F_0 = F$  and the output of the last layer corresponds to the action to be taken at time  $t$ ,  $\mathbf{X}_L = \mathbf{U}_t$  which could be described by a vector of dimension  $F_L = G$ . The GSO  $\mathbf{S}$  to be used in (4) is the one corresponding to the communication network at time  $t$ ,  $\mathbf{S} = \mathbf{S}_t$ . At each layer  $\ell$  we have a bank of  $F_\ell F_{\ell-1}$  filters  $\mathcal{A}_\ell$  described by a set of  $K_\ell F_\ell F_{\ell-1}$  total filter taps  $\{\mathbf{A}_{\ell k}\}_{k=0}^{K_\ell-1}$ .

We note that, in the present framework, we are running one GNN (4) per time instant  $t$ , where each time step is determined by the moment the action is taken and the communication network changes. This implies that we need to carry out  $\sum_{\ell=1}^L (K_\ell - 1)$  total communications before deciding on an action. Therefore, it is important to keep the GNN shallow (small  $L$ ) and the filters short (small  $K_\ell$ ).

In summary, we propose to parametrize the mapping  $\mathcal{F}$  between maps  $\mathbf{Z}_t$  and actions  $\mathbf{U}_t$  by using a GNN (4) acting on observations  $\mathbf{X}_t = \text{CNN}(\mathbf{Z}_t)$  obtained by applying a CNN to the input maps. We note that, by choosing this parametrization we are obtaining a mapping that is naturally distributed and that is adequately exploiting the network structure of the data.

## 5 ARCHITECTURE

The following sections describe the architecture, of which all components are illustrated in Fig. 2.

### 5.1 Processing Observations

In an environment ( $W \times H$ ) with static obstacles, each robot has a local field-of-view (FOV), the size of which is defined by  $\rho$ , beyond which it cannot ‘see’ anything. The data available at each robot is a map  $\mathbf{Z}_t^i$  of size  $W_{FOV} \times H_{FOV}$ . A robot will communicate with other robots within its communication radius  $r$  (Fig. 2 illustrates how we implement such partial observations). The input map  $\mathbf{Z}_t^i$  is fed into a CNN that is run internally on each robot. This results in a vector  $\tilde{\mathbf{x}}_t^i \in \mathbb{R}^F$  containing  $F$  observations (1),  $\tilde{\mathbf{x}}_t^i = \text{CNN}(\mathbf{Z}_t^i)$ . These observations can then be communicated to nearby robots. The intuition behind using a CNN is to process the input map  $\mathbf{Z}_t^i$  into a higher-level feature tensor  $\tilde{\mathbf{x}}_t^i$  describing the observation, goal and states of other robots. This feature tensor is then transmitted via the communication network, as described in the following section, Sec. 5.2.

### 5.2 Communication

Let  $\mathbf{p}_i \in \mathbb{R}^2$  be the global position of robot  $i$  in a given planar workspace. Two robots  $i$  and  $j$  can communicate if  $|\mathbf{p}_i - \mathbf{p}_j| \leq r$

for some given communication radius  $r > 0$ . Each individual robot communicates its compressed observation vector  $\tilde{\mathbf{x}}_t^i$  over the multi-hop communication network, whereby the number of executed hops is limited by  $K$ . As described in Sec. 4.2, we apply our GNN to aggregate and fuse the states ( $\tilde{\mathbf{x}}_t^j$ ) within this  $K$ -hop neighborhood of robots  $j \in \mathcal{N}_i$ , for each robot  $i$ . The output of the communication GNN is a hyper-representation of the fused information of the robot itself and its  $K$ -hop neighbors, which is passed to the action policy, as described in Sec. 5.3. We note that each robot carries a local copy of the GNN, hence resulting in a localized decision-making policy.

### 5.3 Action Policy

We formulate the path-finding problem as a sequential classification problem, whereby an optimal action is chosen at each time step. We adopt a local multi-layer perceptron (MLP) to train our action policy network. More specifically, each node applies a MLP to the aggregated features resulting from the communication GNN. This MLP is the same across all nodes, resembling a weight-sharing scheme. The action  $\tilde{\mathbf{u}}_t^i$  taken by robot  $i$  is computed by a softmax over the probability distribution of motion primitives, which, in our case, consists of five discrete options (up, left, down, right, idle), and are represented by one-hot vectors. The final path is represented by the series of sequential actions.

### 5.4 Network Architecture

In the proposed framework, the CNN architecture is composed by the following set of instructions, Sequential I(32)-Sequential II(32)-Sequential I(64)-Sequential II(64)-Sequential I(128) followed by a Linear-ReLU layer. The instruction Sequential I is composed by the blocks Conv2d-BatchNorm2d-ReLU-MaxPool2d, and Sequential II is the composition of Conv2d-BatchNorm2d-ReLU, where the number in parentheses indicates the number of channels. All kernels are of size 3 with a stride of 1 and zero-padding. In the GNN architecture, we deploy a single layer GNN (as described in Sec. 4.2) and set 128 as the number of input observations  $F$  and output observations  $G$ . Note that we can tune the filter taps  $K$  for non-communication ( $K = 1$ ) and multi-hop communication ( $K > 1$ ). In the action policy, we use a Linear-Softmax layer to decode the output observations  $G$  from GNN with the number of features, 128, into the five motion primitives.

### 5.5 Learning from Expert Data

To train our models, we propose a supervised learning approach based on expert data (i.e., imitation learning). We assume that, at training time, we have access to an optimal trajectory of actions  $\{\mathbf{U}_t^*\}$  for all the robots, and the corresponding maps obtained for this trajectory  $\{\mathbf{Z}_t^i\}$ , collected in a training set  $\mathcal{T} = \{(\{\mathbf{U}_t\}, \{\mathbf{Z}_t^i\})\}$ . Then, we train the mapping  $\mathcal{F}$  so that the output is as close as possible to the corresponding optimal action  $\mathbf{U}^*$ . If the mapping  $\mathcal{F}$  is parametrized in terms of a GNN (4) then this optimization problem becomes

$$\min_{\text{CNN}, \{\mathbf{A}_{\ell k}\}, \text{MLP}} \sum_{(\{\mathbf{U}_t\}, \{\mathbf{Z}_t^i\}) \in \mathcal{T}} \sum_t \|\mathbf{U}_t^* - \mathcal{F}(\{\mathbf{Z}_t^i\}, \mathcal{G}_t)\|. \quad (5)$$

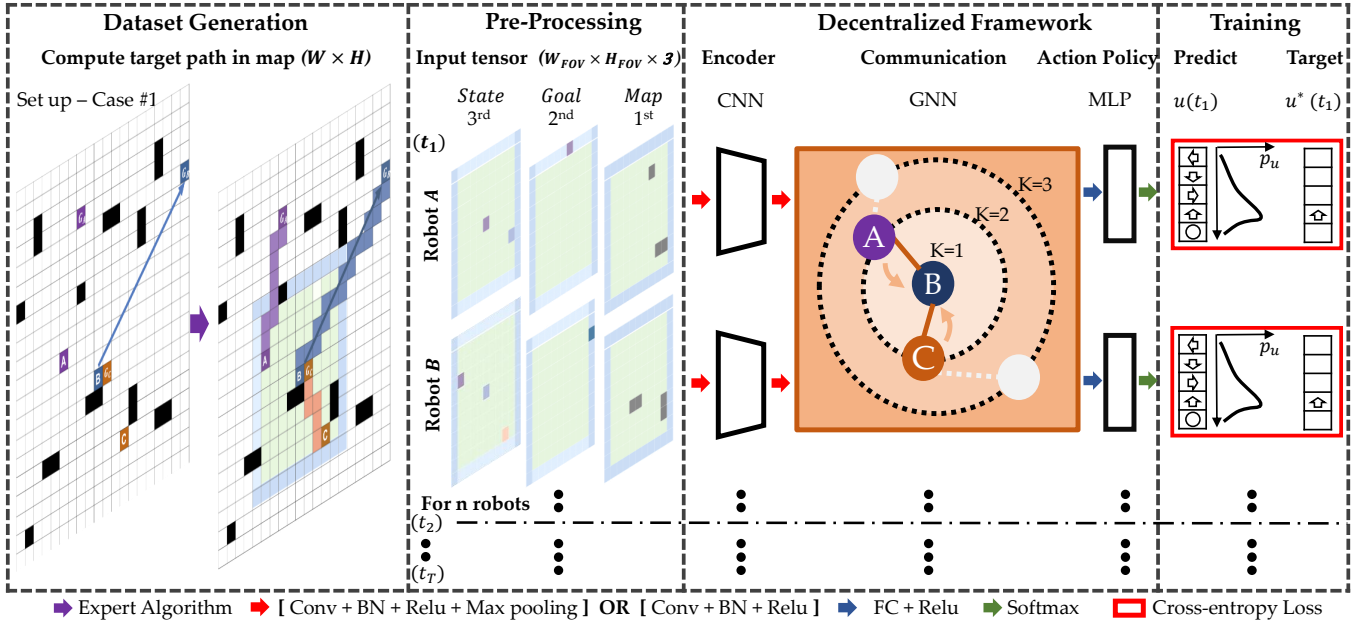


**Figure 2:** Illustration of the proposed framework. (i) The input tensor is based on a binary map representation (1st channel: partial observation of the environment; 2nd channel: the position of goal ( $p_{goal}^i$ ), or its projection onto the boundary of the field-of-view; 3rd channel: self (agent) at center, with other agents within its field-of-view). (ii) The decentralized framework consists of a CNN to extract observations from the input tensor, a GNN to exchange information between the neighboring agents, and an MLP to predict the actions. (iii) Training is performed through cross-entropy loss over a discrete action space.

We are optimizing over the filters in the CNN required to process the map as well as the set of matrices  $\{A_{\ell k}\}$  that contains the  $\sum_{\ell=1}^L K_{\ell} F_{\ell-1} F_{\ell}$  learnable parameters of the communication GNN. Note that the number of parameters is independent of the size of the network  $N$ .

Imitation learning rests on the availability of an optimal solution (further elaborated in Sec. 5.6, below). While this solution might be computationally expensive, or even intractable for large networks, we only need it at training time. Once trained, the GNN models can be deployed in different communication topologies [9], including those with a larger number of robots as is evidenced in the numerical experiments of Sec. 6.4. Given the decentralized nature of the parametrizations, the trained models are efficient in the sense that their computation is distributed among the agents, demanding only communication exchanges with one-hop neighbors.

Training the parametrized mapping  $\mathcal{F}$  through imitation learning guarantees that the actions taken by the individual robots contribute to the global objective of moving the robots towards their pre-specified destination while avoiding collisions with other robots and obstacles. Furthermore, the output actions are computed in a distributed manner.

## 5.6 Expert Data Generation

As described in our problem statement, Sec. 3, the robots operate in a grid world of size  $W \times H$  with static obstacles. We generate random cases, i.e., problem instances, which consist of pairs of start and goal positions for all robots (we also refer to this as a *configuration*). We filter duplicates or invalid cases, and store the remaining cases in a

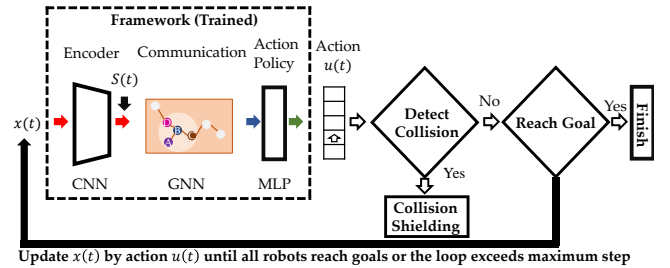


**Figure 3:** Illustration of the inference stage: for each robot, the input tensor  $x$  with same format as in training, is fed to the trained framework to predict its action; collisions are detected and prevented by collision shielding. The input tensor  $x$  is continuously updated until the robot reaches its goal or exceeds maximum steps  $T_{max}$ .

setup pool, which is randomly shuffled at training time. For each case, we generate the optimal solution. Towards this end, we run an expert algorithm: Conflict-Based Search (CBS) [30] (which is a similar approach as taken in [26]). This expert algorithm computes our ‘ground truth paths’ (the sequence of actions for individual robots), within a 300 s timeout, for a given initial configuration. Our data set comprises 30,000 cases for any given grid world and number of agents. This data is divided into a training set (70%), a validation set (15%), and a testing set (15%).

**Algorithm 1:** Generation of sequential actions.

---

**Input:** Input tensor,  $\mathbf{x}_0^i, i \in [0, N]$ ,  $N$  is the number of robots; timeout  $T_{max} = 3T_{MP^*}$  as explained in Sec. 6.1; Policy  $\pi$

**Output:** Predicted paths ( $\hat{\chi}_i$ ) for each robot ( $i$ ), consisting of sequential predicted actions  $\hat{u}_t^i$ , for all  $t \in [0, T_{MP}]$  from initial position  $\mathbf{p}_0^i$

```

1 for  $t$  in  $[0, T_{max}]$  do
2   while not all robots at their goals do
3     for robot  $i \in \{1, \dots, N\}$  do
4       obtain input tensor  $\mathbf{x}_t^i$  and adjacency matrix  $\mathbf{S}_t$ ;
5        $\hat{u}_t^i \leftarrow \pi(\mathbf{x}_t^i, \mathbf{S}_t)$ ;
6       if robot  $i$  with action  $\hat{u}_t^i$  collides with obstacle then
7          $\hat{u}_t^i \leftarrow$  idle (collision shielding);
8       end
9     end
10    if robot  $i$ , with action  $\hat{u}_t^i$ , performs an edge collision
        with robot  $j$  then
11       $\hat{u}_t^i \leftarrow$  idle (collision shielding);
12    else
13      record and update position  $\mathbf{p}_{t+1}^i$  of robot  $i$  by  $\hat{u}_t^i$ ;
14      update input tensor  $\mathbf{x}_t^i$  and adjacency matrix  $\mathbf{S}_t$ .
15    end
16  end
17 end
18 Evaluate  $\hat{\chi}$  according to metrics (Sec. 6.1).
```

---

## 5.7 Policy Execution with Collision Shielding

At inference stage, we execute the action policy with a protective mechanism that we name *collision shielding*. Since it is not guaranteed that robots learn collision-free paths, we require this additional mechanism to guarantee that no collisions take place. Collision shielding is implemented as follows: (i) if the inferred action would result in a collision with another robot or obstacle, then that action is replaced by an idle action; (ii) if the inferred actions of two robots would result in an edge collision (essentially having them swap positions), then those actions are replaced by idle actions. It is entirely possible that robots remain stuck in an idle state until the timeout is reached. When this happens, we count it as a failure case, degrading the measured performance. The overall inference process is summarized in Alg. 1 and Fig. 3.

## 5.8 Dataset Aggregation during Training

The use of collision shielding leads to failure cases due to potential deadlocks in the actions taken by the robots, where some of them remain stuck in an idle state. To overcome such deadlocks, we propose a dataset aggregation method that makes use of an *online expert* (OE) algorithm, during training. More specifically, every  $C$  epochs, we select  $n_{OE}$  random cases from the training set and identify which ones are stuck in a deadlock situation. Then, we run the expert starting from the deadlock configuration in order to unlock them into moving towards their goal. The resulting successful trajectory is added to the training set and this extended training

**Algorithm 2:** Training process with dataset aggregation.

---

**Input:** Input tensor,  $\mathbf{x}_t^i, t \in [0, T_{MP^*}]$ ,  $i \in [0, N]$ ,  $N$  is the number of robots; and adjacency matrix  $\mathbf{S}_t$ ; target actions  $u_t^{*,i}$  generated expert algorithm; cross-entropy loss  $\mathcal{L}$ ; learning rate  $\gamma$ ;  $(\mathbf{x}_t^i, \mathbf{S}_t, u_t^{*,i}) \in$  offline dataset  $D_{offline}$

**Output:** Proposed framework  $\pi(\cdot; w)$

```

1  $D \leftarrow D_{offline}$ ;
2  $\pi(\cdot; \mathbf{w}) \leftarrow$  initialize parameters  $\mathbf{w}$ ;
3 for epoch  $\in \{1, \dots, \text{epoch}_{max}\}$  do
4   for  $\{s_t^i, \mathbf{S}_t, u_t^{*,i}\}_{i=1}^N \in D$  do
5     for  $i \in \{1, \dots, N\}$  do
6        $\hat{u}_t^i = \pi(\mathbf{x}_t^i, \mathbf{S}_t; \mathbf{w})$ ;
7        $\mathbf{w} \leftarrow \mathbf{w} - \gamma \cdot \nabla_{\mathbf{w}} \mathcal{L}(\hat{u}_t^i, u_t^{*,i})$ 
8     end
9   end
10  if mod (epoch, C) = 0 then
11    for  $n_{OE}$  randomly selected cases from  $D_{offline}$  do
12      Deploy  $\pi(\cdot; \mathbf{w})$  based on Alg. 1;
13      Upon timeout, deploy expert algorithm to solve
        failure case  $D_{OE}$ ;
14       $D \leftarrow D \cup D_{OE}$ 
15    end
16  end
17 end
```

---

set is then used in the following epochs. This process is detailed in Alg. 2. We note that no change is made to the validation or test sets. This dataset aggregation method is similar to the approach in DAgger [22], but instead of correcting every failed trajectory, we only correct trajectories from a randomly selected pool of  $n_{OE}$  cases, as calls to our expert algorithm are time-consuming. Another key difference is that we need to resort to an explicit measure of failure (i.e., through the use of a timeout), since focusing on any deviations from the optimal path (as in the DAgger approach) may be misleading, because those paths may still lead to very competitive solutions in our problem setting.

## 6 PERFORMANCE EVALUATION

To evaluate the performance of our method, we perform two sets of experiments, (i) on networks trained and tested on the *same* number of robots, and (ii) on networks trained on a given number of nodes and tested on *previously unseen* team sizes (both larger and smaller).

In Section 6.1 we discuss the performance metrics, in Section 6.2 we present the baseline centralized planner and in Section 6.3 we describe the hardware setup. Section 6.4 presents the results obtained from the proposed framework, evaluated by the corresponding metrics, and compared to the baseline.

### 6.1 Metrics

We consider two key performance metrics:



- **Success Rate** ( $\alpha$ ): A case is considered successful (*complete*) when *all* robots reach their goal prior to the timeout, i.e., when all robots find their paths from  $\mathbf{p}_0^i$  to  $\mathbf{p}_{goal}^i$  for  $i \in [0, N]$ . The success rate is hence quantified by the proportion of successful cases over the total number of tested cases  $n$ :

$$\alpha = \frac{n_{\text{success}}}{n} \quad (6)$$

- **Flowtime Increase** ( $\delta_{FT}$ ): At the end of the system’s inference stage (see Fig. 3), the sequence of actions result in a final path, for each robot. The sum of the executed path lengths ( $FT$ ) may be larger than the sum of expert (target) path lengths ( $FT^*$ ). This deterioration is computed as

$$\delta_{FT} = \frac{FT - FT^*}{FT^*}. \quad (7)$$

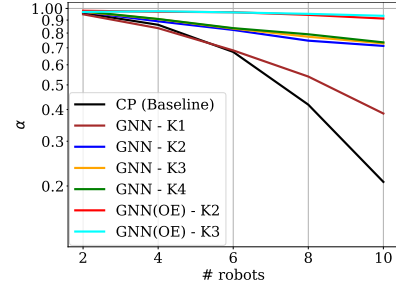
Note that if a robot does not reach its goal, the length of the predicted path is considered to be the length of the maximum allowed path length ( $T_{max} = 3T_{MP^*}$ ). Here,  $T_{MP^*}$  is the makespan of the solution generated by expert algorithm. We also note that computing the flowtime increase with respect to an expert algorithm requires that we can actually solve a case using the expert algorithm in tractable time.

## 6.2 Baseline: Centralized Planner

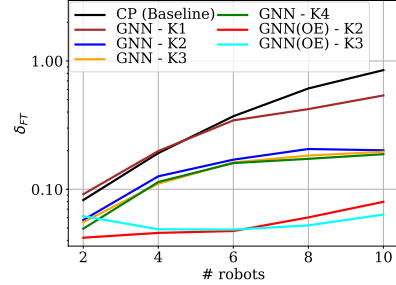
In order to compare our decentralized action policy with a centralized solution, we implement a centralized path planner. For a fair comparison, we train and test this centralized planner on the same data we use for our decentralized policies. The centralized planner (true to its formal definition [30]) receives synchronized global state information (i.e., the states and goals of all robots, at each point in time). Hence, the input tensor ( $W \times H \times (1 + 2 \times N)$ ) consists of the concatenation of the global map ( $W \times H$ , same for all robots), and the goals and initial states ( $W \times H \times 2$ ) in global coordinates for all robots  $i \in [0, N]$ . Convolutional neural networks are applied to process the input tensor ( $\mathbf{x}_i^i$ ). The same CNN architecture as for the decentralized framework (previously described in Sec. 5.4) is used for fair comparison. The main difference to the decentralized architecture is that we use a *multi-output network* to predict the actions ( $\hat{u}_i^i$ ) of all robots simultaneously, instead of an action policy based on exchanged information with nearby agents. Each output-network is a `Linear-Softmax` layer for each individual robot.

## 6.3 Experimental Setup

Our simulations were conducted using a 12-core, 3.2Ghz i7-8700 CPU and an Nvidia GTX 1080Ti GPU with 32 and 11GB of memory, respectively. The proposed network was implemented in PyTorch v1.1.0 [18], and was accelerated with Cuda v10.0 APIs. We used the Adam optimizer [14] with momentum 0.9. The learning rate  $\gamma$  scheduled to decay from  $10^{-3}$  to  $10^{-6}$  within 150 epochs, using cosine annealing. We set the batch size to 64. In the proposed framework, we set L2 regularization as  $10^{-5}$ . The online expert on the GNN is deployed every  $C = 4$  epochs on  $n_{OE} = 500$  randomly selected cases from the training set. In the centralized planner (Sec. 6.2), we set L2 regularization as  $3 \times 10^{-3}$  and kept the optimizer, learning rate, maximum epochs and batch size the same as in the experiments with the GNN.



a: Success rate in GNN



b: Flowtime increase in GNN

**Figure 4:** Results for success rate ( $\alpha$ ) and flowtime increase ( $\delta_{FT}$ ), as a function of the number of robots. Panels (a) and (b) show results for our GNN implementation. For each panel, we vary the number of communication hops ( $K \in [1, 2, 3, 4]$ ), including results obtained through training with online expert (OE) (for  $K = 3$  and  $K = 4$ ). We compare the results with the centralized planner (baseline).

## 6.4 Results

We instantiate a map of size  $20 \times 20$ . The robots’ FOV is  $\rho = 9$ , and the communication radius is  $r = 5$ . The obstacle density is set to 10%, corresponding to the proportion of occupied over free space in the environment. At each time step, each robot runs a forwards pass of its local action policy (i.e., the trained network). At the end of each case (i.e., it is either solved or the timeout is reached), we record the length of each robot’s path and the number of robots that reach their goals, to compute performance metrics according to Sec. 6.1.

### 6.4.1 Effect of Communication on Flowtime and Success Rates.

Figures 4a and 4b show results for the success rate and flowtime increase, respectively, as a function of the number of robots. For each panel, we train a model for  $N \in [2, 3, 6, 8, 10]$ , and test it on instances of the same robot team size. In each experiment, we vary the number of communication hops ( $K \in [1, 2, 3, 4]$ ). We compare the results with the centralized planner (as a baseline). Note that for  $K = 1$  there are no communications involved.

In both figures, we see a drop in performance for larger teams, but this drop is much more pronounced for both the centralized planner (CP) and the non-communicative GNN ( $K = 1$ ). There is a small but noticeable improvement as we increase the communication hop count, in particular for the implementation with the online expert (as described in Sec. 5.8).

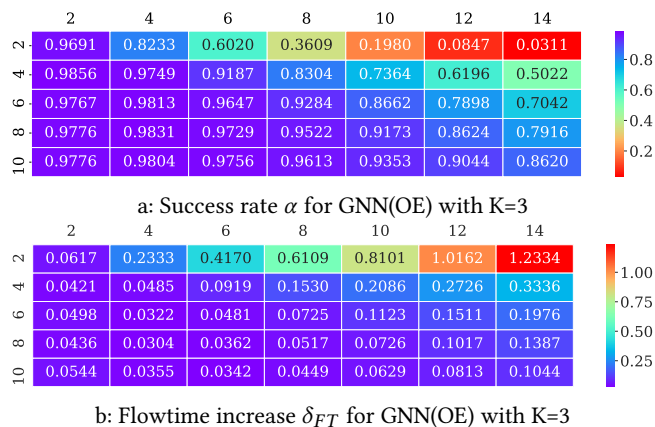


**Figure 5:** Success rate and flowtime increase (trained with OE, for  $K = 3$ ). The rows represent the number of robots on which each model was trained, and columns represent the number of robots at test time. In other words, the values on the diagonal are the values for environments with the same number of robots during test and training. The generalization performance of the network is visualized by a heatmap, which maps performance values into a color range from purple to red, where purple indicates the best performance and red indicates the worst performance.

**6.4.2 Generalization.** Tables 5a and 5b summarize the generalization capability of our model for success rate and flowtime increase, respectively. The experiment was carried out by testing networks across previously unseen cases. The tables specify the number of robots *trained on* in the rows, and the number of robots *tested on* in the columns.

The generalization performance of the network is visualized by a heatmap, which maps performance values into a color range from purple to red, where purple indicates the best performance and red indicates the worst performance. By comparing across rows under the same column, we see that when tested on the same number of robots (i.e., column), the network trained on a larger number of robots tends to perform better (even better than on the same instance size as trained on), leading to higher success rates and lower flowtime increases. Also, comparing performance across columns for a fixed row, we observe that as we train networks with increasingly large robot teams, the network tends to generalize better across any unseen instances (larger as well as smaller robot teams).

We perform subsequent experiments on larger robot teams to further test the generalization. We train a GNN ( $K = 3$ ) network with the online expert on 10 robots, and test it on 20 and 40 robots in  $28 \times 28$  and  $40 \times 40$  environments, respectively (gridmaps are scaled to preserve the same effective density). Different from our success rate metric, which only considers complete cases (all robots reach their goals), Fig. 6 presents the proportion of cases distributed over the number of robots reaching their goals. The distributions show that, in both cases, more than 50% of all robots *always* reach their goals, and in 70% of cases, more than 80% of robots reach their goals. For instance, in the 20-robot example, in 395 of 500 cases (79%), at least 16 robots reach their goals. In the 40-robot example, in 141 of 200 cases (70.5%), at least 32 robots reach their goals.

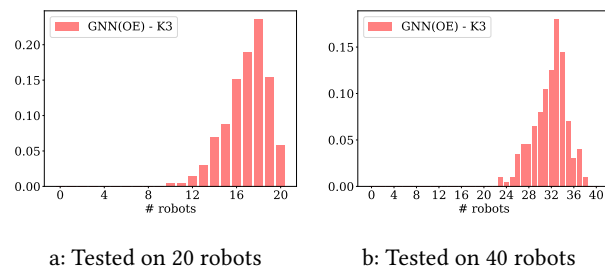


**Figure 6:** Histogram of proportion of cases distributed over the number of robots reaching their goal; the network is trained on 10 robots, and tested on 20 and 40 robots respectively with hop count  $K = 3$ , employing OE.

## 7 DISCUSSION AND FUTURE WORK

The intrinsic limitations of the centralized planner (CP) are that it requires a larger network capacity (as described in Sec. 6.2), and that it needs to be re-trained for *each new number of robots*  $N$  (i.e., it does not have the capability of generalizing across robot team sizes). Moreover, as the results in Fig. 4 demonstrate, it exhibits a steep performance decrease for growing robot team sizes; this weakness can potentially be mitigated by increasing the network capacity, but clearly, this strategy does not scale.

In contrast, our decentralized framework generalizes to different numbers of robots, as seen in Sec. 6.4.1 and Sec. 6.4.2. With communication ( $K > 1$ ), the network performs more stably than the centralized (CP) and non-communicative GNN ( $K = 1$ ) as the number of robots increases. We note that the centralized solution [30], implemented in C++, can compute the solution for a given case in less than 0.02 s for 8 agents. However, a centralized unit is required to obtain the states and goals of all robots, and to broadcast back a solution. In contrast, a single forward pass of our model (enabling a robot to predict its action) takes only  $0.0019 \pm 2.15e^{-4}$  s on the workstation described in Sec. 6.3. In addition to the decentralized nature of our solution, this speed of computation is beneficial in real-world deployments, where each robot runs its own (localized) action policy. We note that, in contrast, the expert algorithm [30] is intractable for more than 14 agents in dense environments within the given timeout; this is corroborated by results in [2, 26].

The experiment in Sec. 6.4.2 showed the capability of our decentralized policy to generalize to robot teams of larger scales. Table 5a and Table 5b showed that the framework trained in smaller robot teams ( $n = 2, 4$ ) tends to perform worse than those trained in larger teams ( $n = 6, 8, 10$ ), across any unseen instances (larger as well as smaller in size). The intuition for the cause of this phenomenon can be due to two main factors. Firstly, larger robot teams tend to cause more collisions, allowing the policy to learn how to plan more efficient paths more quickly. Secondly, policies trained on very small robot teams (e.g. 2 robots), tend to produce communication topologies that are idiosyncratic, and hence, may generalize more poorly.

We also demonstrated that the use of our online expert leads to significant improvements (as seen in Fig. 4). The Appendix includes further evidence confirming this tendency. Fig. 8 shows how the GNN with the online expert was able to compute the paths for all robots in several instances, given 32 robots, whereas the pure GNN



implementation (without data aggregation) could not. Moreover, a significant right-shift of the distribution is visible.

There are some assumptions and corresponding limitations in the current implementation, which will be improved in future work. Firstly, we assumed that communication between robots was achieved instantly without delay. Time-delayed aggregation GNNs [36] can be introduced to extend our framework to handle the time-delayed scenario.

Secondly, inter-robot collisions, especially position swaps, are the main reason causing the lower success rates for larger teams. However, the current decentralized policy was only able to learn collision-avoidance implicitly from the solution of the expert algorithm. The optimal planner tends to avoid inter-robot collision several steps ahead through collision-based search. This artifact reduces the number of ‘interesting’ cases in our training set, where collisions happen in coming steps. One potential solution to this is to deploy a policy gradient to add a penalty on the action causing a collision. However, such a strategy (e.g., as implemented in [26]) is harder to train, and is left for future work.

## 8 CONCLUSIONS

We considered the problem of collision-free navigation in multi-robot systems where the robots are restricted in observation and communication range. We proposed a combined architecture, composed of a convolutional neural network that extracts adequate features from local observations, and a graph neural network that communicates these features among robots. The key idea behind our approach is that we jointly trained these two components, enabling the system to best determine what information is relevant for the team of robots as a whole. We devised a data aggregation strategy (through an online expert) that facilitated faster learning. We performed experiments in cluttered environments with robot teams of varying sizes, and measured the success rates and sum of costs over the resulting planned paths. The results demonstrated the validity of our approach; in particular, we showed our model’s capability to generalize to previously unseen cases involving much larger robot teams.

This work is the first to apply GNNs to the problem of multi-robot path planning. Our results show that we are very close to achieving the same performance as first-principles-based methods. Of particular importance is that fact that we can already scale our system to sizes that are intractable for coupled centralized solvers, while remaining computationally feasible through our decentralized approach.

## 9 ACKNOWLEDGMENTS

We gratefully acknowledge the support of ARL grant DCIST CRA W911NF-17-2-0181. A. Prorok was supported by the Engineering and Physical Sciences Research Council (grant EP/S015493/1). We gratefully acknowledge their support.

## REFERENCES

- [1] Javier Alonso-Mora, Andreas Breitenmoser, Paul Beardsley, and Roland Siegwart. 2012. Reciprocal collision avoidance for multiple car-like robots. In *Robotics and Automation (ICRA), 2012 IEEE International Conference on*. IEEE, 360–366.
- [2] Max Barer, Guni Sharon, Roni Stern, and Ariel Felner. 2014. Suboptimal variants of the conflict-based search algorithm for the multi-agent pathfinding problem. In *Seventh Annual Symposium on Combinatorial Search*.
- [3] Peter Battaglia, Razvan Pascanu, Matthew Lai, Danilo Jimenez Rezende, and others. 2016. Interaction networks for learning about objects, relations and physics. In *Advances in Neural Information Processing Systems (NIPS)*. 4502–4510.
- [4] Vishnu R Desaraju and Jonathan P How. 2012. Decentralized path planning for multi-agent teams with complex constraints. *Autonomous Robots* 32, 4 (2012), 385–403.
- [5] David K Duvenaud, Dougal Maclaurin, Jorge Iparraguirre, Rafael Bombarell, Timothy Hirzel, Alán Aspuru-Guzik, and Ryan P Adams. 2015. Convolutional networks on graphs for learning molecular fingerprints. In *Advances in Neural Information Processing Systems (NIPS)*. 2224–2232.
- [6] John Enright and Peter R Wurman. 2011. Optimization and coordinated autonomy in mobile fulfillment systems.. In *Automated action planning for autonomous mobile robots*. 33–38.
- [7] M. Everett, Y. F. Chen, and J. P. How. 2018. Motion Planning Among Dynamic, Decision-Making Agents with Deep Reinforcement Learning. In *2018 IEEE/RSJ International Conference on Intelligent Robots and Systems (IROS)*. 3052–3059. <https://doi.org/10.1109/IROS.2018.8593871>
- [8] Cornelia Ferner, Glenn Wagner, and Howie Choset. 2013. ODRM\*: Optimal multirobot path planning in low dimensional search spaces. In *IEEE International Conference Robotics and Automation (ICRA)*. 3854–3859.
- [9] F. Gama, J. Bruna, and A. Ribeiro. 2019. Stability Properties of Graph Neural Networks. *arXiv:1905.04497v2 [cs.LG]* (4 Sep. 2019). <http://arxiv.org/abs/1905.04497>
- [10] F. Gama, A. G. Marques, G. Leus, and A. Ribeiro. 2019. Convolutional Neural Network Architectures for Signals Supported on Graphs. *IEEE Trans. Signal Process.* 67, 4 (Feb. 2019), 1034–1049.
- [11] Justin Gilmer, Samuel S Schoenholz, Patrick F Riley, Oriol Vinyals, and George E Dahl. 2017. Neural message passing for quantum chemistry. *Proceedings of the 34th International Conference on Machine Learning* 70 (2017).
- [12] Pasquale Grippa, Doris A Behrens, Christian Bettstetter, and Friederike Wall. 2017. Job selection in a network of autonomous UAVs for delivery of goods. *Robotics: Science and Systems* (2017).
- [13] A. Heimowitz and Y. C. Eldar. 2017. A Unified View of Diffusion Maps and Signal Processing on Graphs. In *2017 Int. Conf. Sampling Theory and Appl.* IEEE, Tallinn, Estonia, 308–312.
- [14] Diederik P Kingma and Jimmy Ba. 2014. Adam: A method for stochastic optimization. *arXiv preprint arXiv:1412.6980* (2014).
- [15] Yugang Liu and Goldie Nejat. 2013. Robotic urban search and rescue: A survey from the control perspective. *Journal of Intelligent & Robotic Systems* 72, 2 (2013), 147–165.
- [16] Laëticia Matignon, Laurent Jeanpierre, and Abdel-Ilhah Mouaddib. 2012. Coordinated multi-robot exploration under communication constraints using decentralized markov decision processes. In *Twenty-sixth AAAI conference on artificial intelligence*.
- [17] A. Ortega, P. Frossard, J. Kovačević, J. M. F. Moura, and P. Vandergheynst. 2018. Graph Signal Processing: Overview, Challenges and Applications. *Proc. IEEE* 106, 5 (May 2018), 808–828.
- [18] Adam Paszke, Sam Gross, Soumith Chintala, Gregory Chanan, Edward Yang, Zachary DeVito, Zeming Lin, Alban Desmaison, Luca Antiga, and Adam Lerer. 2017. Automatic Differentiation in PyTorch. In *NIPS Autodiff Workshop*. Advances in Neural Information Processing Systems, Long Beach, CA, USA, 1–4.
- [19] Amanda Prorok. 2018. Graph Neural Networks for Learning Robot Team Coordination. *Federated AI for Robotics Workshop, IJCAI-ECAL/ICML/AAMAS 2018*; *arXiv:1805.03737 [cs]* (May 2018). <http://arxiv.org/abs/1805.03737> arXiv: 1805.03737.
- [20] Amanda Prorok and Vijay Kumar. 2017. Privacy-preserving vehicle assignment for mobility-on-demand systems. In *2017 IEEE/RSJ International Conference on Intelligent Robots and Systems (IROS)*. IEEE, 1869–1876.
- [21] Aravind Rajeswaran, Kendall Lowrey, Emanuel V. Todorov, and Sham M Kakade. 2017. Towards Generalization and Simplicity in Continuous Control. In *Advances in Neural Information Processing Systems (NIPS)*, I. Guyon, U. V. Luxburg, S. Bengio, H. Wallach, R. Fergus, S. Vishwanathan, and R. Garnett (Eds.). 6550–6561. <http://papers.nips.cc/paper/7233-towards-generalization-and-simplicity-in-continuous-control.pdf>
- [22] Stéphane Ross, Geoffrey Gordon, and Drew Bagnell. 2011. A reduction of imitation learning and structured prediction to no-regret online learning. In *Proceedings of the fourteenth international conference on artificial intelligence and statistics*. 627–635.
- [23] M. Rotkowitz and S. Lall. 2005. A characterization of convex problems in decentralized control. *IEEE Trans. Automat. Control* 50, 12 (Dec. 2005), 1984–1996. <https://doi.org/10.1109/TAC.2005.860365>
- [24] A. Sandryhaila and J. M. F. Moura. 2013. Discrete Signal Processing on Graphs. *IEEE Trans. Signal Process.* 61, 7 (April 2013), 1644–1656.
- [25] Guillaume Sartoretti, Justin Kerr, Yunfei Shi, Glenn Wagner, TK Kumar, Sven Koenig, and Howie Choset. 2019. PRIMAL: Pathfinding via Reinforcement and Imitation Multi-Agent Learning. *IEEE Robotics and Automation Letters* 4 (2019), 2378–2385. Issue 3.

- [26] G. A. Sartoretti, J. Kerr, Y. Shi, G. Wagner, T. K. S. Kumar, S. Koenig, and H. Choset. 2019. PRIMAL: Pathfinding via Reinforcement and Imitation Multi-Agent Learning. *IEEE Robotics and Automation Letters* (2019), 1–1. <https://doi.org/10.1109/LRA.2019.2903261>
- [27] Franco Scarselli, Marco Gori, Ah Chung Tsoi, Markus Hagenbuchner, and Gabriele Monfardini. 2009. The graph neural network model. *IEEE Transactions on Neural Networks* 20, 1 (2009), 61–80.
- [28] Tom Schouwenaars, Bart De Moor, Eric Feron, and Jonathan How. 2001. Mixed integer programming for multi-vehicle path planning. In *European Control Conference (ECC)*. IEEE, 2603–2608.
- [29] Guni Sharon, Roni Stern, Ariel Felner, and Nathan R Sturtevant. 2015. Conflict-based search for optimal multi-agent pathfinding. *Artificial Intelligence* 219 (2015), 40–66.
- [30] Guni Sharon, Roni Stern, Ariel Felner, and Nathan R Sturtevant. 2015. Conflict-based search for optimal multi-agent pathfinding. *Artificial Intelligence* 219 (2015), 40–66.
- [31] D. I Shuman, S. K. Narang, P. Frossard, A. Ortega, and P. Vandergheynst. 2013. The Emerging Field of Signal Processing on Graphs: Extending high-dimensional data analysis to networks and other irregular domains. *IEEE Signal Process. Mag.* 30, 3 (May 2013), 83–98.
- [32] David Silver. 2005. Cooperative Pathfinding. *Artificial Intelligence and Interactive Digital Entertainment* 1 (2005), 117–122.
- [33] Kevin Spieser, Samitha Samaranyake, Wolfgang Gruel, and E Frazolli. 2016. Shared-vehicle mobility-on-demand systems: a fleet operator’s guide to rebalancing empty vehicles. In *Transportation Research Board*.
- [34] Trevor Standley and Richard Korf. 2011. Complete Algorithms for Cooperative Pathfinding Problems. In *Proceedings of the Twenty-Second International Joint Conference on Artificial Intelligence - Volume Volume One (IJCAI’11)*. AAAI Press, Barcelona, Catalonia, Spain, Article 1, 6 pages. <https://doi.org/10.5591/978-1-57735-516-8/IJCAI11-118>
- [35] J. Tobin, R. Fong, A. Ray, J. Schneider, W. Zaremba, and P. Abbeel. 2017. Domain randomization for transferring deep neural networks from simulation to the real world. In *2017 IEEE/RSJ International Conference on Intelligent Robots and Systems (IROS)*. 23–30. <https://doi.org/10.1109/IROS.2017.8202133>
- [36] E. Tolstaya, F. Gama, J. Paulos, G. Pappas, V. Kumar, and A. Ribeiro. 2019. Learning Decentralized Controllers for Robot Swarms with Graph Neural Networks. In *Conf. Robot Learning 2019*. Int. Found. Robotics Res., Osaka, Japan.
- [37] Jur Van Den Berg, Stephen J Guy, Ming Lin, and Dinesh Manocha. 2011. Reciprocal n-body collision avoidance. In *Robotics research*. Springer, Berlin, Heidelberg, 3–19.
- [38] Jur Van den Berg, Ming Lin, and Dinesh Manocha. 2008. Reciprocal velocity obstacles for real-time multi-agent navigation. In *IEEE International Conference on Robotics and Automation (ICRA)*. IEEE, 1928–1935.
- [39] J. P. van den Berg and M. H. Overmars. 2005. Prioritized motion planning for multiple robots. In *2005 IEEE/RSJ International Conference on Intelligent Robots and Systems*. IEEE, Edmonton, Alta., Canada, 430–435. <https://doi.org/10.1109/IROS.2005.1545306>
- [40] Y. Wang, N. Matni, and J. C. Doyle. 2018. Separable and Localized System-Level Synthesis for Large-Scale Systems. *IEEE Trans. Automat. Control* 63, 12 (Dec. 2018), 4234–4249. <https://doi.org/10.1109/TAC.2018.2819246>
- [41] Wenying Wu, Subhrajit Bhattacharya, and Amanda Prorok. 2019. Multi-Robot Path Deconfliction through Prioritization by Path Prospects. *arXiv:1908.02361 [cs]* (Aug. 2019). <http://arxiv.org/abs/1908.02361> arXiv: 1908.02361.
- [42] Jingjin Yu and Steven M LaValle. 2013. Structure and intractability of optimal multi-robot path planning on graphs. In *AAAI*.
- [43] Jingjin Yu and Steven M. LaValle. 2015. Optimal Multi-Robot Path Planning on Graphs: Complete Algorithms and Effective Heuristics. *arXiv:1507.03290 [cs]* (July 2015). <http://arxiv.org/abs/1507.03290> arXiv: 1507.03290.

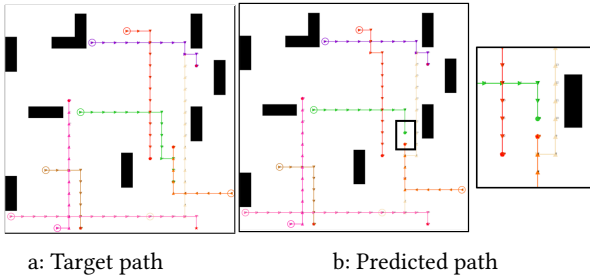


**Figure 7:** Demo of the path of individual robots. Panel (a) illustrates the target path of expert algorithm, and Panel (b) illustrates the predicted path from the network without online expert is trained and tested on 8 robots. Note that, the deadlock caused by collision shielding is zoom in aside(b).

### A SUPPLEMENTARY RESULTS

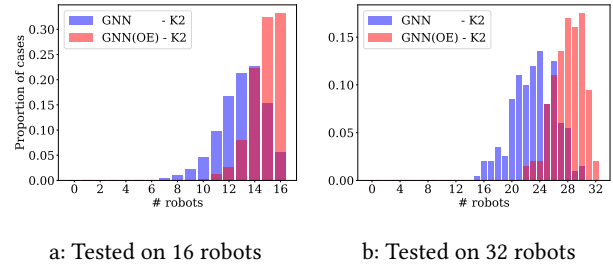
This appendix presents supplementary material for our approach. Fig. 7 exemplifies a typical failure case caused by inter-robot collision (i.e., in this case, a position-swap). Fig. 8 compares the GNN performance with and without the online expert (OE). We also investigate the impact of filter taps  $K$  (Fig. 9).

Fig. 7 illustrates the target path computed by the expert algorithm and the path computed by the network trained and tested on 8 robots. Different from a search-based method, the proposed framework can not explore the future collision ahead of time. This results in the inter-robot collision in Fig. 7 (b). Although the collision shielding can force robots to remain idle, the lack of solutions for such scenarios (e.g., position-swap) in the offline data-set causes the deadlock. This yields the need for an online expert (through a data-set aggregation method, as described in Sec. 5.8) that provides a solution from this configuration onward.

To further evaluate the improvement provided by the online expert, we trained the GNN with and without the online expert, and tested the networks on 16 and 32 robots in  $28 \times 28$  and  $40 \times 40$  environments. Fig. 8 shows a distribution shift from the GNN without the online expert to the GNN with the online expert. We see how the GNN network with the online expert tends to generalize better than the one without, since the proportion of robots reaching

the goal is significantly larger. This holds for tests on 16 and 32 robots, indicating the network starts to learn how to solve those cases that the GNN network without the online expert could not solve.

To evaluate the impact of filter taps ( $K$ ), we increases the hop count  $K$  from 2 into 3 in our experiment of testing 20 and 40 robots. We observed the proportion of robots reaching the goal slightly increases from  $K = 2$  into 3 in Fig. 9.



**Figure 8:** Histogram of proportion of cases distributed over the number of robots reaching their goal; the network is trained on 8 robots and tested on 16 robots in (a), and tested on 32 robots in (b). Panels (a) and (b) use hop count  $K = 2$  without and with online expert, respectively.

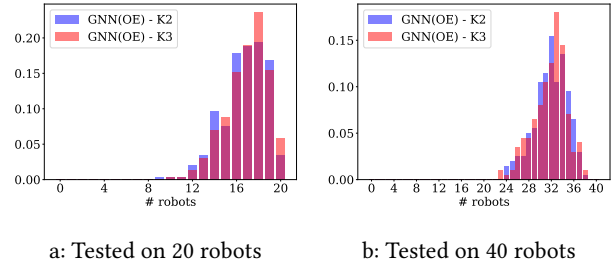


**Figure 9:** Histogram of proportion of cases distributed over the number of robots reaching their goal; the network is trained on 10 robots and tested on 20 robots in (a), and tested on 40 robots in (b). Panels (a) and (b) use hop count  $K = 2$  and  $K = 3$  with online expert, respectively.